ARMY RESEARCH LABORATORY

A Comparison of the Deformation Flow and Failure of Two Tungsten Heavy Alloys in Ballistic Impacts

by Brian E. Schuster, Bryan P. Peterson, and Lee S. Magness

ARL-RP-122 **May 2006**

A reprint from the *Proceedings of the Sixth International Conference on Tungsten, Refractory & Hardmetals*, sponsored by the Metal Powder Industries Federation in cooperation with the Refractory Metals Association and APMI International, pp. 350–358, 7–8 February 2006, Sheraton World Resort, Orlando, FL.

Reprinted with permission from *Tungsten, Refractory & Hardmetals VI*, Metal Powder Industries Federation, 105 College Road East, Princeton, NJ, 2006.

NOTICES

Disclaimers

The findings in this report are not to be construed as an official Department of the Army position unless so designated by other authorized documents.

Citation of manufacturer's or trade names does not constitute an official endorsement or approval of the use thereof.

Destroy this report when it is no longer needed. Do not return it to the originator.

Army Research Laboratory

Aberdeen Proving Ground, MD 21005-5066

ARL-RP-122 **May 2006**

A Comparison of the Deformation Flow and Failure of Two Tungsten Heavy Alloys in Ballistic Impacts

Brian E. Schuster, Bryan P. Peterson, and Lee S. Magness
Weapons and Materials Research Directorate, ARL

A reprint from the *Proceedings of the Sixth International Conference on Tungsten, Refractory & Hardmetals,* sponsored by the Metal Powder Industries Federation in cooperation with the Refractory Metals Association and APMI International, pp. 350–358, 7–8 February 2006, Sheraton World Resort, Orlando, FL.

Reprinted with permission from *Tungsten, Refractory & Hardmetals VI,* Metal Powder Industries Federation, 105 College Road East, Princeton, NJ, 2006.

REPORT DOCUMENTATION PAGE

Form Approved
OMB No. 0704-0188

1. REPORT DATE *(DD-MM-YYYY)*	2. REPORT TYPE	3. DATES COVERED (From - To)
May 2006	Final	January 2005–December 2005

4. TITLE AND SUBTITLE
A Comparison of the Deformation Flow and Failure of Two Tungsten Heavy Alloys in Ballistic Impacts

5a. CONTRACT NUMBER

5b. GRANT NUMBER

5c. PROGRAM ELEMENT NUMBER

6. AUTHOR(S)
Brian E. Schuster, Bryan P. Peterson, and Lee S. Magness

5d. PROJECT NUMBER
58T8G7

5e. TASK NUMBER

5f. WORK UNIT NUMBER

7. PERFORMING ORGANIZATION NAME(S) AND ADDRESS(ES)
U.S. Army Research Laboratory
ATTN: AMSRD-ARL-WM-TC
Aberdeen Proving Ground, MD 21005-5066

8. PERFORMING ORGANIZATION REPORT NUMBER
ARL-RP-122

9. SPONSORING/MONITORING AGENCY NAME(S) AND ADDRESS(ES)

10. SPONSOR/MONITOR'S ACRONYM(S)

11. SPONSOR/MONITOR'S REPORT NUMBER(S)

12. DISTRIBUTION/AVAILABILITY STATEMENT
Approved for public release; distribution is unlimited.

13. SUPPLEMENTARY NOTES
A reprint from the *Proceedings of the Sixth International Conference on Tungsten, Refractory & Hardmetals*, sponsored by the Metal Powder Industries Federation in cooperation with the Refractory Metals Association and APMI International, 7–8 February 2006, Sheraton World Resort, Orlando, FL.

14. ABSTRACT
Ballistic tests were conducted with sub-scale long rod penetrators of two different processing conditions of the same tungsten heavy alloy. The liquid-phase sintered composite of 90% tungsten-9% nickel-1% cobalt (by weight) was tested in its low-strength, as-sintered and heat-treated condition, and in a high strength, 50% cold-worked (by swaging) and aged condition. Small, but consistent, differences in the ballistic performances of the two lots of penetrators were observed in depth of penetration tests in thick armor steel targets and in limit velocity determinations against finite thickness steel targets.

Metallographic examinations were conducted on the residual penetrators recovered from sectioned steel targets. Using the tungsten particles in the nickel alloy matrices of these residual penetrator materials as embedded strain gauges, the strain distributions, deformation gradients, and flow and failure behaviors of these two tungsten heavy alloy lots were examined. Correlations were sought between the flow and failure behaviors of these two lots and their ballistic performances.

15. SUBJECT TERMS
tungsten, deformation, flow, alloys, ballistic impacts

16. SECURITY CLASSIFICATION OF:			17. LIMITATION OF ABSTRACT	18. NUMBER OF PAGES	19a. NAME OF RESPONSIBLE PERSON
a. REPORT	b. ABSTRACT	c. THIS PAGE			Brian E. Schuster
UNCLASSIFIED	UNCLASSIFIED	UNCLASSIFIED	UL	16	19b. TELEPHONE NUMBER (*Include area code*) 410-278-6733

A Comparison of the Deformation, Flow, and Failure of Two Tungsten Heavy Alloys

Brian E. Schuster, Bryan P. Peterson and Lee S. Magness
US Army Research Laboratory
AMSRD-ARL-WM-TC
Aberdeen Proving Ground
Aberdeen MD 21005-5066

ABSTRACT

Ballistic tests were conducted with sub-scale long rod penetrators of two different processing conditions of the same tungsten heavy alloy. The liquid-phase sintered composite of 90% tungsten-9% nickel-1% cobalt (by weight) was tested in its low-strength, as-sintered and heat-treated condition, and in a high-strength, 50% cold-worked (by swaging) and aged condition. Small, but consistent, differences in the ballistic performances of the two lots of penetrators were observed in depth of penetration tests in thick armor steel targets and in limit velocity determinations against finite thickness steel targets.

Metallographic examinations were conducted on the residual penetrators recovered from sectioned steel targets. Using the tungsten particles in the nickel alloy matrices of these residual penetrator materials as embedded strain gauges, the strain distributions, deformation gradients, and flow and failure behaviors of these two tungsten heavy alloy lots were examined. Correlations were sought between the flow and failure behaviors of these two lots and their ballistic performances.

INTRODUCTION

Tungsten heavy alloys (WHA) have been used as replacement alloys for depleted uranium (DU) based kinetic energy penetrators (KEP). These alloys typically consist of particles of tungsten that are surrounded by a matrix with differing composition. While the mechanical properties of these alloys can be altered dramatically with changes in the cold-work, heat-treatment, tungsten content and matrix composition, this generally results in little change in the ballistic performance of the composite alloy. As reported by Leonard and Magness [1], the differences in ballistic performance of WHA penetrator materials of a given density are usually on the order of the experimental errors. In this study, two extreme conditions of a liquid-phase sintered composite of 90% tungsten-9% nickel-1% (90W9Ni1Co) cobalt were examined. The high-strength swaged and aged condition consistently achieved greater penetration depth at a given impact velocity and required lower velocities to perforate a given thickness of armor than the low-strength, as-sintered and heat-treated condition. When large differences in penetration performance have been observed between WHA's and DU alloys of comparable density, differences in the flow and failure behavior were demonstrated in the metallographic examinations of the residual penetrators [7]. Similarly, penetrators of the 2 conditions of 90W9Ni1Co were examined for a similar correlation between flow and failure behavior and ballistic performance.

BALLISTIC COMPARISON

Two lots of 90% W-9 % nickel-1% cobalt (by weight), with densities of 17.25 g/cm^3 were manufactured by GTE Sylvania, Inc. (now Osram-Sylvania, Inc.). Both lots received a post-sinter heat-treatment to re-solutionize a W_4Ni intermetallic compound [2]. Lot 1 was left in the as-sintered and heat-treated condition, while lot 2 underwent additional cold-work of 50 % reduction-in-area (RA) by swaging, followed by an aging heat-treatment (3 hours at 600°C). These lots of 90W9Ni1Co represent the extreme cases in processing and properties of conventional WHA's with a summary shown in table 1. The heavily worked swaged lot showed a dramatic increase in both the yield strength and ultimate strength of the material; the yield strength is 2 ½ times larger than the unworked condition, and there is a smaller, yet significant, difference in the peak strength (1000 vs. 1641 MPa ultimate strengths). At the very high strain rates occurring during ballistic impacts, the flow stresses of both alloys will be higher, but their differences can be expected to be much smaller [Meyer et al (3), Coates and Ramesh (4)]. In either case, the flow stress of the WHA penetrator material will be greatly exceeded by the shear stresses and hydrostatic pressures imposed on the head of the long rod penetrator during ballistic impact.

Table 1. Quasistatic Properties and Ballistic Performance of 90 W - 9 Ni - 1 Co

Material	*Rockwell C Hardness*	*Yield Strength -0.20% [MPa]*	*Ultimate Strength [MPa]*	*Elongation to Failure [%]*	*Unnotched Charpy Energy* [J]*	*Limit Velocities vs. 76.2mm RHA Plate [m/s]*	
						L/D = 15	*L/D = 20*
Lot 1 As-Sintered & Heat-Treated	32	614	1000	34	89	1380	1330
Lot 2 Swaged 50% RA Aged	49.9	1530	1641	7	12	1340	1290

* Charpy values for 5 mm by 5mm bars

Table 1. Quasi-Static Properties and Ballistic Limit Velocities of the as-sintered and swaged WHA.

For each lot of material, the bar stock was machined to hemispherical nosed, 65 gram long rod penetrators with length-to-diameter (L/D) ratios of 15 and 20. Penetrators of each lot and L/D ratio were shot into 76.2 mm (3 in) rolled homogeneous armor (RHA) plates [6] at normal incidence to determine the ballistic limit velocity i.e., the lowest velocity required to perforate a given target [5]. The results of the ballistic tests are also reported in table 1. The swaged and aged WHA lot consistently delivered a 40 m/s improvement in the ballistic limit velocity when compared to the as-sintered counterpart for both the L/D 15 and 20 penetrators. The 40 m/s shift in limit velocities is much larger than is typically observed between WHA's of equal density. The difference in quasi-static flow strength alone can not explain the difference in ballistic performance.

Metallographic examinations were conducted to examine the flow and failure behaviors of the residual penetrators of these two WHA lots.

STRAIN MEASUREMENTS FROM RESIDUAL PENETRATORS

Residual penetrators from each lot of WHA were selected for metallographic analysis. These residual penetrator blocks were sectioned along the centerline of the penetration tunnel. These blocks were then polished using standard metallographic techniques, beginning with silicon-carbide paper, followed by several iterations of diamond paste, and a final polish of 0.1 μm. A JEOL-6460LV Scanning Electron Microscope was used for an in-depth examination of the flow of these two lots of WHA.

The microstructures of the two lots of WHA, in essentially their original state, are visible in figures 1(a) and (b) and at the back of the residual penetrators in figures 2(a) and 3(a). The as-sintered WHA microstructure consists of nearly spherical W particles that are surrounded by the Ni-Co matrix. The 50% swaged WHA instead contains higher aspect ratio (ratio of major and minor axes) tungsten particles that are elongated along the rod axis by swaging. The observation of this difference in the aspect ratio for the as-sintered and swaged conditions suggested that the W particles could be used as a sort of imbedded strain gauge. In this example, the overall reduction in area produces an approximately homogeneous deformation resulting in an increased aspect ratio along the penetrator's axis. The aspect ratio of the W particles could then be used to map out the strain distributions within the entire residual penetrator. Examinations of the periphery of the mushroomed head of the residual penetrators, and the microstructures within the discarded chips (erosion products) from the head of the penetrator, could provide a quantitative analysis of the flow and subsequent failure of the material in the penetration process.

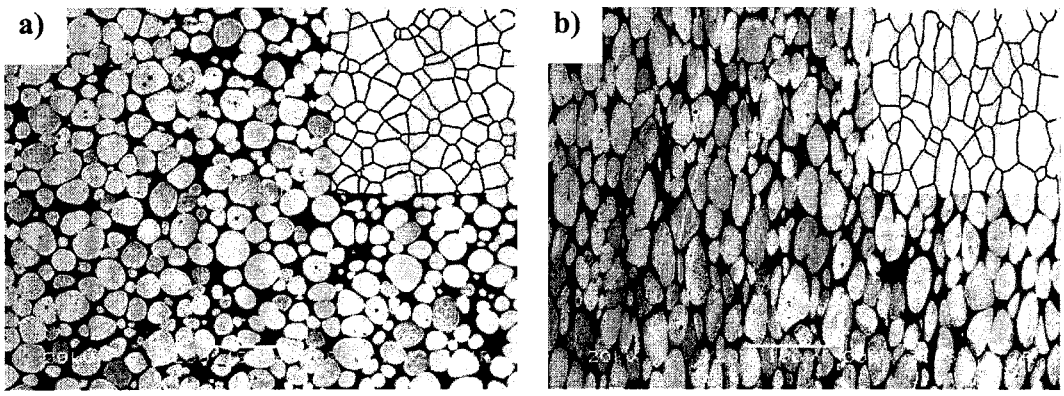

Figure 1. Initial microstructures of the as-sintered (a) and swaged lots (b) of WHA. The inset of each shows the idealized trace microstructures used for automated strain measurements.

The strain of a tungsten particle can be calculated with some simple assumptions. An assumption is made that initially the W particle is spherical with radius r. This is assumed to deform to an elliptical form with some aspect ratio, s, where s is equal to the ratio of the major axis, $2a$, and the minor axis, $2b$ (note: a and b are

respectively the semimajor and semiminor axes of the ellipse). The equivalent area calculation would equate the cross-sectional area of the initial state, πr^2 , and final state, πab . The true strain, ε ,can then be calculated as follows:

$$\varepsilon = \ln \frac{a}{r} = \ln \frac{a}{\sqrt{ab}} = \frac{1}{2} \ln s$$

While this provides some estimate to the strain of the particles, there are some limitations to this technique. Initially, the tungsten particles are nearly, but not exactly, spherical. A measurement of the microstructure shown in figure 1(a) has an average aspect ratio of 1.4, with a random orientation of the major axes of the individual particles. For a quick comparison, the swaged microstructure in figure 1(b) has a mean aspect ratio of 2.32, and therefore a true strain of 42%. This underestimates the 50% overall reduction of area in the material, but this should be expected as the overall deformation of the material includes contributions from the softer Ni-Co matrix surrounding the higher strength W particles.

In a previous study, manual measurements of the W particles were used to analyze the deformation of these penetrators [8]. In this study, automated routines are applied to measure the aspect ratio, and therefore the strain, of many thousands of tungsten particles across large portions of the residual penetrator. Edge detection routines were used in Image Pro Plus 5.0 to isolate the W phase from the matrix in the backscattered electron SEM micrographs. The considerable contiguity between adjacent W particles was problematic for isolation of individual W particles, even when using edge detection and automatic particle splitting routines. A second routine was applied to build a trace of the individual particles. This allowed for rapid manual splitting of the individual particles with a reference back to the original microstructure. Figure 1(a) and (b) show typical starting micrographs with the processed image or the trace microstructures shown as an inset. From this trace microstructure, automated measurements of particle area, major axis, minor axis, and particle aspect ratio were collected. These measures were then related back to the approximate strain using the method previously outlined.

METALLOGRAPHIC EXAMINATION OF RESIDUAL PENETRATORS

The macroscopic view of the as-sintered and swaged residual penetrators is shown in figures 2(a) and 3(b), respectively. During the penetration process, the rear of the penetrator essentially remains undeformed. The evolution in microstructure from this initial state to that found in the discarded chip is most evident in figure 2(b), where it is observed that the tungsten particles are gradually elongated from the original microstructure into a very high aspect ratio structure. Extremely elongated W particles are found throughout the discarded chips. The microstructure found in figure 2(c) is typical of those observed in the chips. Contrast this behavior with that shown figure 3 for the swaged lot of WHA. It appears that the deformation localizes more quickly leading to the shear chips found in figures 3(b) and (c). The calculated strains for a radial slice of the residual penetrator are shown in color coded form in Figure 4.

For each penetrator, strain measurements were taken from the microstructures shown in figures 2(b), 3(b), and 3(c). Trace microstructures were created from these selected areas of the residual penetrators. For the as-sintered case, the strains were computed assuming an initial aspect ratio of 1.4. The calculated strains for a radial slice of the residual penetrator are shown in color coded form in figure 4. For the swaged penetrator, the strains were computed using an average initial aspect ratio of 2.32. The corresponding color-coded strain distributions for a radial slice of the residual swaged penetrator and one of the discarded chips are shown in figures 5(a) and 5(b).

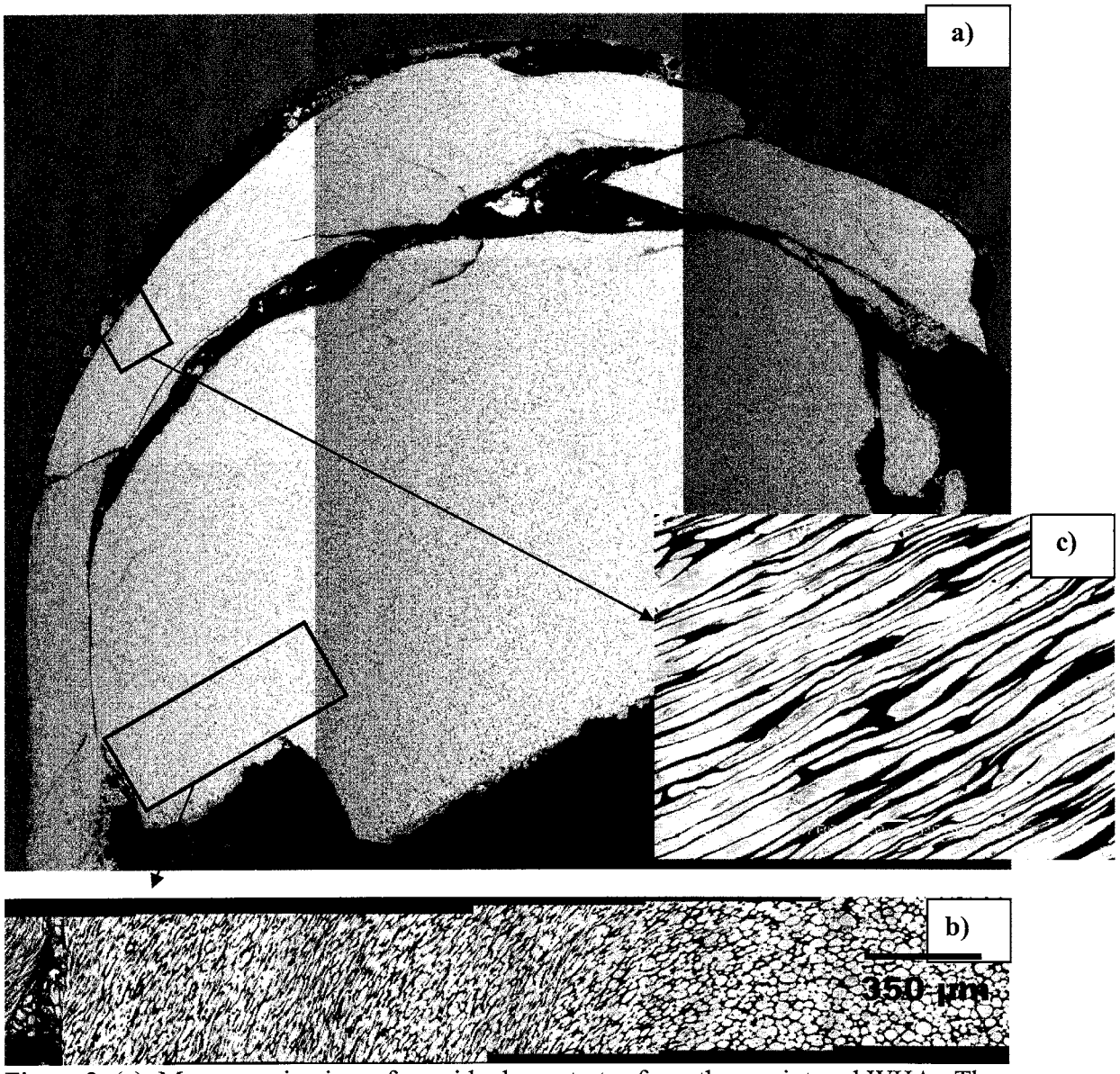

Figure 2. (a) Macroscopic view of a residual penetrator from the as-sintered WHA. The inset view in (b) shows the evolution of the microstructure from the undeformed state to the highly elongated structure that is found in (c).

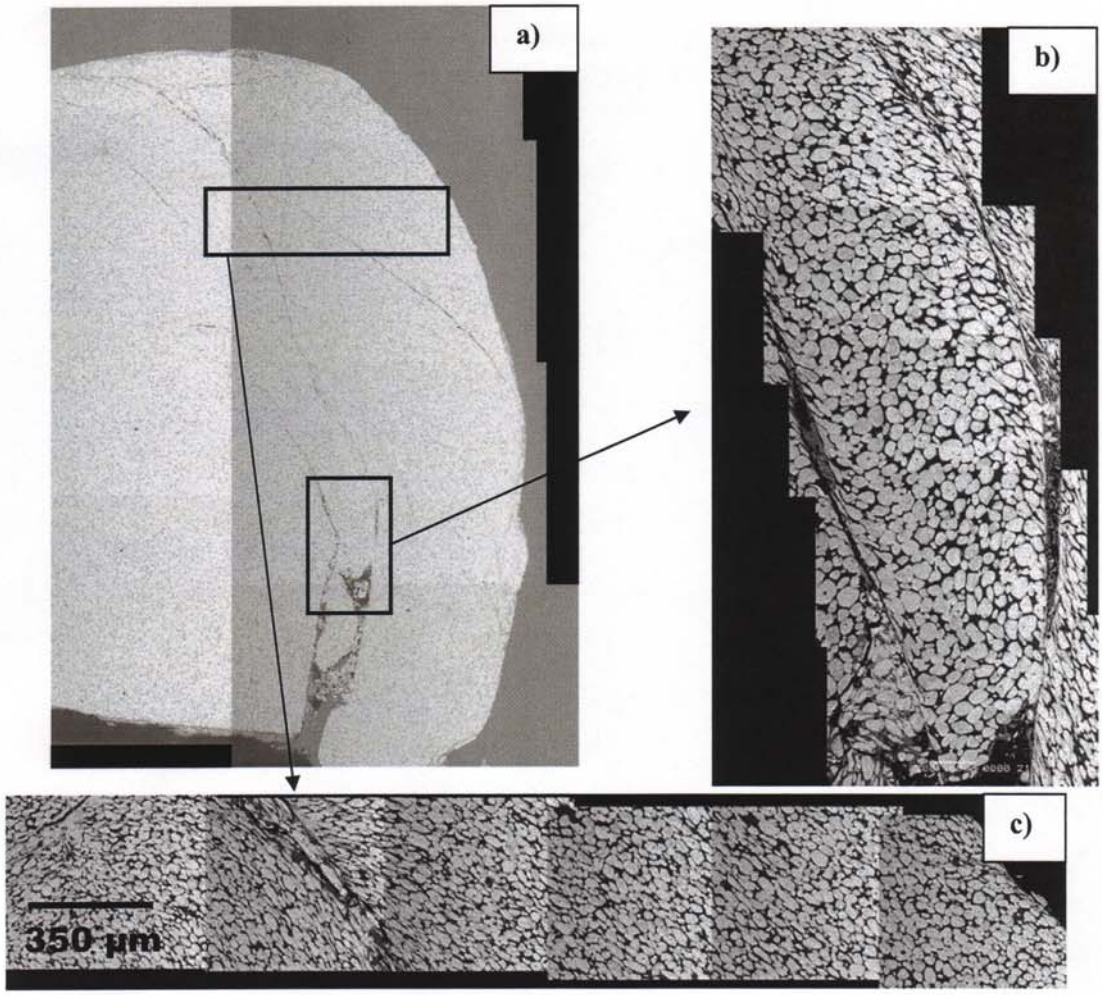

Figure 3. (a) Macroscopic view of a penetrator from the swaged lot of WHA with enlarged views of the discarded chips found in (b) and (c).

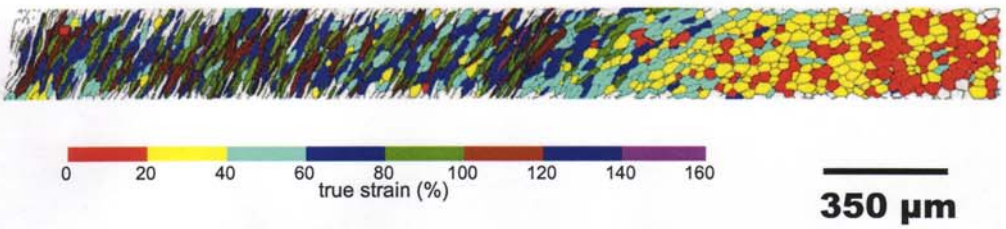

Figure 4. This selected area strain measurement from the as-sintered residual penetrator is based on figure 2b. Strains were calculated from the measurements of the final W particle aspect ratio assuming an initial aspect ratio of 1.4.

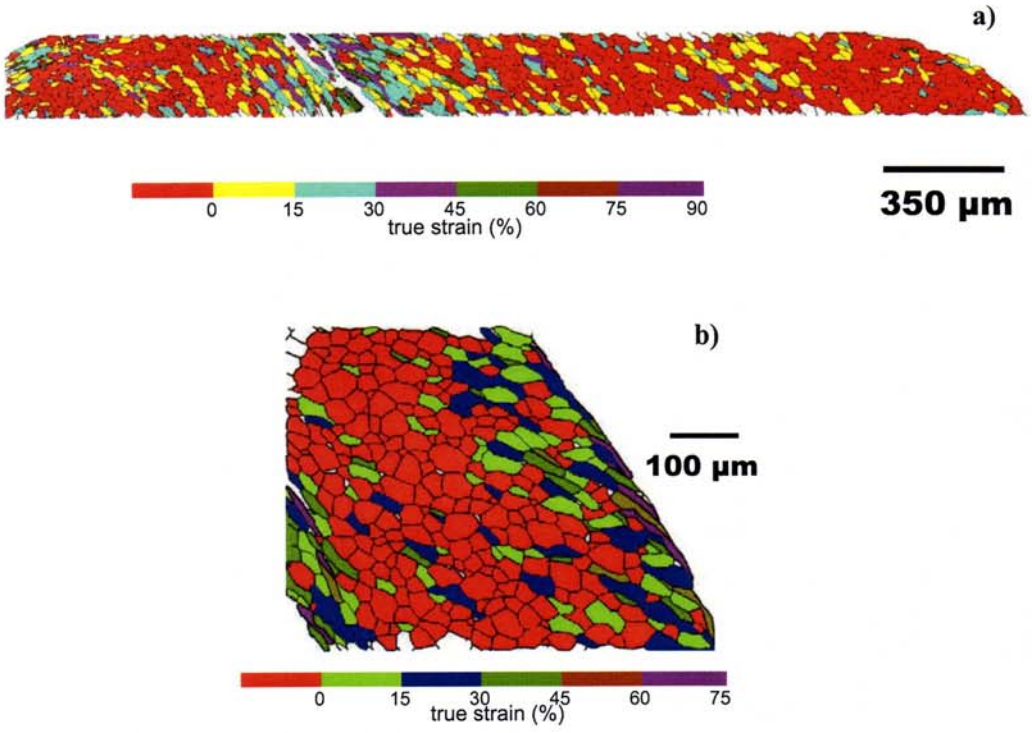

Figure 5. Selected area strain measurements from the swaged WHA penetrator. Strains were calculated from the measurements of the final W particle aspect ratio assuming an initial aspect ratio of 2.32 where (a) is adapted from figure 3(c) and (b).

DISCUSSION

From a macroscopic view, there are apparent differences in the flow and failure of the two lots of WHA. The as-sintered lot shows the classic mushroomed head of the penetrator with very stable flow; i.e., there is no sign of flow localizations throughout the penetrator. The discarded chips show very uniform, high aspect ratio tungsten particles with strains that exceed 150%. From figures 2(b) and 4, the evolution to this elongated structure becomes very apparent. Moving right-to-left across figure 4, the original microstructure is gradually elongated over a length of several millimeters to form the needle-like structure of the particles found from the middle to extreme left side of the figure. A measurement of the mean strain found in figure 4 yields an average strain of 70% in this field of view.

This is in great contrast to the swaged material. Throughout many of the discarded chips of the swaged microstructure, it appears that much of the original microstructure is retained. The discarded chips of the swaged penetrator shows regions of highly localized deformation (shear bands) across a length of a few hundred micrometers, bounded by low aspect ratio grains that are similar in appearance to the original microstructure. Measurements taken through the shear bands found in 5(a) and (b) show

an average aspect ratio of 3.5, relating to an average estimate of strain of roughly 20% (using an aspect ratio of 2.32 as a starting point and zero strain). The material outside the band has an average aspect ratio of 2.1, meaning that through the bulk of the material within the discarded chips had undergone compressive deformation (more spherodized appearance) rather than being highly elongated as is typical of the as-sintered WHA.

The calculated strain values mentioned above illustrate that there are complicating factors in the strain analysis of the swaged WHA penetrator. Prior to the ballistic test, the W particles in the swaged WHA begin with an already high (2.32 on average) aspect ratio, with an average preferred orientation parallel to the penetrator rod axis (corresponding to the rod axis during swaging). During the ballistic impact, the WHA material is first compressively loaded along the rod axis then increasingly undergoes a transverse shearing deformation as the rod forms the mushroomed head and is inverted (or back extruded) from the forward moving penetrator target interface. Along the centerline of the penetrator, essentially only axial loading is applied and the original 2.32 aspect ratio W particles are compressed, reversing the prior their deformation. The swaged W particles first return to their original un-swaged appearance (average aspect ratio of 1.4 with a random orientation) and then continue to flatten, increasing in aspect ratio with a radial average orientation. As one moves away from the rod axis, however, transverse loads combined with the axial loads produce different deformation paths.

For the swaged WHA, this post-mortem analysis of the strain says little about the actual strain history of a grain. The initial and final forms of the grains are known. The problem arises in that a grain that has been compressed from a 2.32:1 ratio to a 1:1 ratio and then eventually elongated to 2.32:1 is assumed to have the same strain as a particle that remains at an aspect ratio of 2.32 throughout the deformation process. This strain progression is largely missing from the as-sintered case where the grains are gradually elongated, rather than initially compressed. While a correction factor could be applied to the case of the swaged material, it is not clear if this initial compression is homogeneous throughout the head of the penetrator. While the measurements from the swaged condition underestimate the overall deformation, it is more important to note that the strain gradients and the spacing between strain localizations remain unchanged. This is the important characteristic of the deformation that leads to the improved ballistic behavior. The swaged material undergoes localized plastic deformation with rapid discard of the shear chips. This is in stark contrast to the as-sintered penetrators which undergo very stable, homogeneous deformation leading to late discard of the chips.

CONCLUSIONS

Cold-work of 50% RA (by swaging), followed by an aging heat treatment, improved the penetration performance of a liquid-phase sintered 90W-9Ni-1Co composite into steel armor. Sub-scale, long rod penetrators of this heavily-worked alloy perforated a monolithic RHA steel target plate at velocities 30 to 40 m/s lower than for equivalent mass and geometry rods of the same alloy in the unworked condition. Metallographic examinations were conducted on the residual penetrators recovered from the ballistic tests. Significant differences were observed in the distributions of the plastic deformation

within the "mushroomed" heads that formed on the two sets of penetrators, in the number and the location of plastic localizations (shear bands) within the heads, and the level of microstructural deformation that occurred between the localizations. The deformation of the unworked lot of WHA penetrator material was more diffuse; i.e., more broadly distributed throughout the mushroomed head with less distinctive plastic localizations. The deformation of the worked lot of WHA penetrator material appears to focus more quickly into plastic localizations, resulting in less deformation within the chips of WHA discarded from the head of the penetrator. The differences in the flow and failure behaviors of these two lots of the 90W-9Ni-1Co alloy are consistent with the 30 to 40 m/s shift in their limit velocities.

REFERENCES

1. W. Leonard, L. Magness, and D. Kapoor, "Improving Mechanical Properties of Tungsten heavy Alloy Composites Through Thermomechanical Processing," *Int. Conf. on Tungsten & Tungsten Alloys, MPIF*, 1992, p.127
2. T. Myhre, "Processing Description for Cold-Worked 90% Tungsten Alloy Rods," Union Carbide Corp.- Nuclear Div. Report Y/PG-2275 (1979)
3. L. Meyer, F. Behler, K. Frank, and L. Magness, "Interdependencies Between the Dynamic Mechanical Properties and the Ballistic Behavior of Materials," *Proc. 12th Int. Symp. Ballistics* 1990
4. R. Coates and K.T. Ramesh, "The Rate-Dependent Deformation of a Tungsten Heavy Alloy," *Mat. Sci. & Eng. A*, vol 145, 1991, p.159
5. J. Lambert and G. Jonas, "Towards Standardization in Terminal Ballistics Testing: Velocity Representation," U.S. Army Ballistic Research Laboratory Report, ARBRL-R-1852, (1976)
6. MIL-A-12560G(MR), Armor Plate, Steel, Wrought, Homogeneous (1984)
7. L. Magness and T. Farrand , "Deformation Behavior and Its Relationship to the Penetration Performance of High-Density KE Penetrator Materials," US Army Science Conf, (1990) 149
8. B.E. Schuster and L.S. Magness "A Comparison of the Flow and Failure of Two WHAs in Ballistic Imapact" *P/M Sci. & Tech. Briefs*, vol. 5 , 2003, pp. 26-30

NO. OF
COPIES ORGANIZATION

1 (PDF ONLY) DEFENSE TECHNICAL INFORMATION CTR
DTIC OCA
8725 JOHN J KINGMAN RD
STE 0944
FORT BELVOIR VA 22060-6218

1 US ARMY RSRCH DEV & ENGRG CMD
SYSTEMS OF SYSTEMS INTEGRATION
AMSRD SS T
6000 6TH ST STE 100
FORT BELVOIR VA 22060-5608

1 INST FOR ADVNCD TCHNLGY
THE UNIV OF TEXAS
AT AUSTIN
3925 W BRAKER LN
AUSTIN TX 78759-5316

1 DIRECTOR
US ARMY RESEARCH LAB
IMNE ALC IMS
2800 POWDER MILL RD
ADELPHI MD 20783-1197

3 DIRECTOR
US ARMY RESEARCH LAB
AMSRD ARL CI OK TL
2800 POWDER MILL RD
ADELPHI MD 20783-1197

ABERDEEN PROVING GROUND

1 DIR USARL
AMSRD ARL CI OK TP (BLDG 4600)

NO. OF
COPIES ORGANIZATION

ABERDEEN PROVING GROUND

3 DIR USARL
AMSRD ARL WM TC
R COATES
L MAGNESS
B SORENSEN

INTENTIONALLY LEFT BLANK.